Archival Report

Biological Psychiatry: GOS

Partial or Complete Loss of Norepinephrine Differentially Alters Contextual Fear and Catecholamine Release Dynamics in Hippocampal CA1

Leslie R. Wilson, Nicholas W. Plummer, Irina Y. Evsyukova, Daniela Patino, Casey L. Stewart, Kathleen G. Smith, Kathryn S. Konrad, Sydney A. Fry, Alex L. Deal, Victor W. Kilonzo, Sambit Panda, Natale R. Sciolino, Jesse D. Cushman, and Patricia Jensen

ABSTRACT

BACKGROUND: Contextual fear learning is heavily dependent on the hippocampus. Despite evidence that catecholamines contribute to contextual encoding and memory retrieval, the precise temporal dynamics of their release in the hippocampus during behavior is unknown. In addition, new animal models are required to probe the effects of altered catecholamine synthesis on release dynamics and contextual learning.

METHODS: We generated 2 new mouse models of altered locus coeruleus–norepinephrine (NE) synthesis and utilized them together with $GRAB_{NE}$ and $GRAB_{DA}$ sensors and in vivo fiber photometry to investigate NE and dopamine (DA) release dynamics in the dorsal hippocampal CA1 during contextual fear conditioning.

RESULTS: Aversive foot shock increased both NE and DA release in the dorsal CA1, while freezing behavior associated with recall of fear memory was accompanied by decreased release. Moreover, we found that freezing at the recent time point was sensitive to both partial and complete loss of locus coeruleus–NE synthesis throughout prenatal and postnatal development, similar to previous observations of mice with global loss of NE synthesis beginning postnatally. In contrast, freezing at the remote time point was compromised only by complete loss of locus coeruleus–NE synthesis beginning prenatally.

CONCLUSIONS: Overall, these findings provide novel insights into the role of NE in contextual fear and the precise temporal dynamics of both NE and DA during freezing behavior and highlight complex relationships between genotype, sex, and NE signaling.

https://doi.org/10.1016/j.bpsgos.2023.10.001

Contextual learning involves the integration of the multisensory features of a particular environment into a single representation that can support complex adaptive behaviors (1–3). Individual stimuli can have substantially different meaning and significance in different contexts, and contexts themselves can serve as powerful predictors of appetitive and aversive events. In contextual fear conditioning, the multisensory features that define the conditioning chamber are associated with an aversive unconditioned stimulus that subsequently drives fear expression (3–6). Contextual fear is heavily dependent on the hippocampus (7,8), and numerous studies have demonstrated the importance of norepinephrine (NE) and dopamine (DA) signaling in different hippocampal subregions to contextual encoding and retrieval (9–16).

With respect to NE, the hippocampus receives virtually all of its inputs from the locus coeruleus (LC) (17,18), and LC-NE signaling to dorsal hippocampal area CA1 (dCA1) has been specifically implicated in retrieval of contextual memories (19,20). LC-NE signaling through β-adrenergic receptors has been shown to modulate activation of dCA1 pyramidal neurons during memory retrieval (11), and optogenetic activation of LC-NE inputs to the dCA1 enhances subsequent retrieval of contextual memories 24 hours after training (21). Consistent with these observations, global loss of NE synthesis in dopamine β-hydroxylase knockout mice (Dbh^{ko}) (22) results in deficits in short-term memory retrieval (11). Despite these important discoveries, the precise temporal dynamics of NE and DA release in the dCA1 during fear conditioning remain unknown. In addition, it is unclear how catecholamine dynamics and freezing behavior during contextual fear are altered by more subtle disruptions of NE synthesis.

In the current study, we present 2 new mouse models of disrupted LC-NE synthesis beginning prenatally: a hypomorphic allele of *Dbh* that results in reduced NE in central noradrenergic neurons and an LC conditional knockout with total loss of NE in the LC and reduced NE in other central noradrenergic nuclei. Utilizing these mice in conjunction with a preexposure-dependent contextual fear assay (23,24) and

ISSN: 2667-1743

in vivo fiber photometry in the dCA1, we sought to determine the effects of partial and complete embryonic loss of LC-NE synthesis on freezing behavior and assess NE and DA release dynamics during 4 phases of the contextual fear assay. Our data identify deficits in freezing behavior and unique patterns of catecholamine release dynamics in the dCA1 that are differentially sensitive to partial or complete embryonic loss of NE.

METHODS AND MATERIALS

Animals

All procedures related to animal use were approved by the Animal Care and Use Committee of the National Institute of Environmental Health Sciences. Mice were group housed and maintained on a 12-hour light/dark cycle at 72 ± 2 °F with access to food and water ad libitum.

To establish the $Dbh^{tm2.2Pjen}$ (Dbh^{flx}) mouse line, a targeting vector was electroporated into G4 embryonic stem cells (25), and chimeras were bred to C57BL/6J mice. All mice used in the study were backcrossed to C57BL/6J >10 generations. For details on targeting vector construction, genotyping, and crosses, see Supplemental Methods and Materials.

Immunohistochemistry/Mass Spectrometry/ Droplet Digital Polymerase Chain Reaction

For immunohistochemistry, tissue was collected, and immunofluorescent labeling was performed as previously described (26). For catecholamine analysis, 100 to 200 μL of whole blood, hippocampal samples, and adrenals were flash frozen and processed for mass spectrometry. For quantification of Dbh and tyrosine hydroxylase (Th) messenger RNA (mRNA), RNA was collected from the pons, medulla, adrenal, and stellate ganglion and analyzed by droplet digital polymerase chain reaction (PCR). For details, see Supplemental Methods and Materials.

In Vivo Fiber Photometry/Fear Conditioning

AAVs (adeno-associated viruses) expressing tdTomato (27) and NE (28) or DA (29) sensor were unilaterally injected in the dCA1. Mice were tested in a fear conditioning chamber with a grid floor (Med Associates), and freezing behavior was assessed using Ethovision XT software version 16 (Noldus Information Technology). Sensor and tdTomato fluorescence intensities were measured using a custom-built fiber photometry system (30). See Supplemental Methods and Materials for detailed procedures and analyses.

RESULTS

Generation of a Mouse Model of Disrupted LC-NE Synthesis

In previous studies using Dbh^{ko} mice, the embryonic lethality believed to be caused by loss of NE synthesis in the peripheral nervous system was overcome by dosing pregnant dams with L-DOPS, thus permitting *Dbh*-independent NE synthesis during prenatal development (22,31). Consequently, Dbh^{ko} mice lack global NE postnatally after L-DOPS treatment is withdrawn. While the Dbh^{ko} is an excellent model to assess the requirement for NE throughout the postnatal period, the restoration of NE synthesis mediated by L-DOPS may obscure phenotypes associated with prenatal loss of NE. To eliminate LC-NE synthesis beginning in embryonic development and avoid the prenatal lethality associated with global loss of *Dbh*, we generated a Cre-dependent conditional knockout allele, $Dbh^{tm2.2Pjen}$ (Dbh^{flx}), in which fluorescent tags allow recombination to be monitored in noradrenergic neurons (Figure 1A; Figure S1). In the absence of Cre-mediated recombination, transcription from the Dbh^{flx} allele will produce mRNA encoding separate DBH and tdTomato proteins. Cre-mediated recombination will delete most of the *Dbh* coding sequence, leaving a mutant allele (Dbh^{null}) that encodes a fusion between exon 1 and EGFP (enhanced green fluorescent protein). Thus, if Cre is expressed in a subset of noradrenergic neurons, the Cre+ noradrenergic neurons can be identified by EGFP fluorescence, while Cre-negative noradrenergic neurons that retain DBH activity are labeled with tdTomato. To confirm that recombination occurs as expected, we crossed Dbh^{flx} heterozygotes with $Tmem163^{Tg(ACTB-cre)2Mrt}$ mice (32) which exhibit ubiquitous Cre activity. PCR analysis of genomic DNA demonstrated Cre-dependent deletion of the sequence between the 2 loxP sites (Figure 1A).

Next, we selectively eliminated NE synthesis in LC neurons by taking advantage of the fact that the anatomically defined LC (within the central gray of the pons, adjacent to the fourth ventricle), together with a rostral portion of the adjacent dorsal subcoeruleus, is uniquely defined by embryonic expression of the transcription factor *En1* (engrailed 1) and later expression of *Dbh* (18). Because *En1* is expressed before *Dbh*, the LC neurons of mice heterozygous for $En1^{Cre}$ (33) and homozygous for Dbh^{flx} ($Dbh^{LC\text{-}null}$ mice) (Figure 1B) will never produce DBH protein and therefore never synthesize NE. As expected, $Dbh^{LC\text{-}null}$ mice were viable, and LC noradrenergic neurons of $Dbh^{LC\text{-}null}$ mice were labeled with EGFP, indicating loss of *Dbh* expression (Figure 1C). In non-LC noradrenergic neurons, we observed tdTomato, indicating the unrecombined allele (Figure 1C). EGFP was fainter than tdTomato, and detection of both fluorophores required immunofluorescent labeling; nevertheless, these results indicate that the fluorescent tags can be used to monitor Cre-dependent recombination of Dbh^{flx}.

Mutation of a Putative Transcriptional Enhancer Is Associated With Reduced *Dbh* mRNA Expression

To confirm that $Dbh^{LC\text{-}null}$ mice lack *Dbh* expression in the LC, we performed co-immunofluorescent labeling of DBH and TH. Consistent with the recombination data, DBH was not detected in the LC of $Dbh^{LC\text{-}null}$ mice (Figure 2A). We observed no differences in DBH labeling between Cre+ and Cre-negative $Dbh^{wt/wt}$ controls and no genotype-specific differences in TH labeling. However, in Cre-negative $Dbh^{flx/flx}$ mice, DBH labeling appeared qualitatively weaker than in $Dbh^{wt/wt}$ controls (Figure 2A).

Next, we examined NE tissue content in the hippocampus, which receives virtually all of its noradrenergic inputs from the LC, using mass spectrometry. As expected, NE was absent in the hippocampus of $Dbh^{LC\text{-}null}$ mice (Figure 2B). Consistent with DBH immunolabeling, we observed an approximately

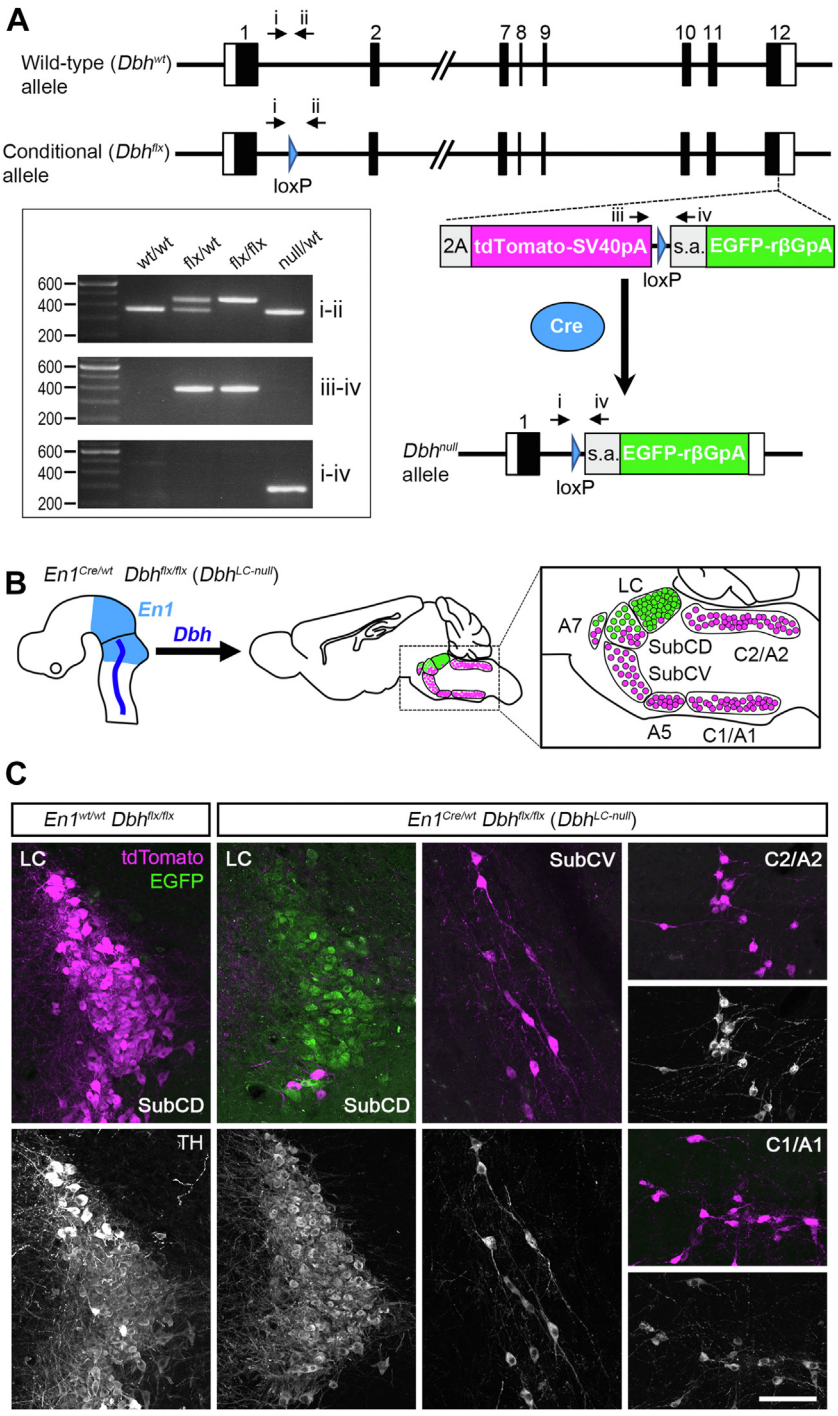

Figure 1. Conditional knockout allele of the mouse *Dbh* gene. **(A)** Schematic diagram showing the wild-type and modified *Dbh* locus. Coding exons are indicated by black boxes, 5′ and 3′ untranslated regions by white boxes, and introns by black lines. In the conditional (Dbh^{flx}) allele, a single loxP site is inserted within intron 1, and a larger insertion in exon 12 consists of 2A peptide (56), tdTomato complementary DNA, SV40 polyadenylation signal, loxP, splice acceptor sequence, EGFP complementary DNA, and rabbit β-globin polyadenylation signal. After Cre recombination, the null allele consists of exon 1, a chimeric intron consisting of the 5′ portion of intron 1 and the exogenous splice acceptor, and EGFP. Arrows indicate polymerase chain reaction primers flanking the loxP sites. Box: Polymerase chain reaction analysis of genomic DNA from $Dbh^{wt/wt}$ (wild-type), heterozygous $Dbh^{flx/wt}$, homozygous $Dbh^{flx/flx}$, and heterozygous $Dbh^{null/wt}$ mice demonstrates excision of exons 2–12 and the tdTomato cassette following Cre recombination. **(B)** Sagittal schematic diagram of the embryonic neural tube showing overlap of noradrenergic progenitors and *En1* expression domain in the anterior hindbrain and adult sagittal schematic showing location of noradrenergic nuclei and expected fluorescent labeling of noradrenergic neurons in $Dbh^{LC\text{-}null}$ ($En1^{Cre/wt}$ $Dbh^{flx/flx}$). **(C)** Representative coronal sections from Cre-negative $Dbh^{flx/flx}$ and $Dbh^{LC\text{-}null}$ mice showing tdTomato or EGFP expression in neurons of the LC, SubCD, SubCV, C2/A2, and C1/A1 nuclei (top panel of each image pair). TH immunoreactivity confirms noradrenergic identity of labeled neurons (bottom panel of each image pair). Scale bar = 100 μm. EGFP, enhanced green fluorescent protein; LC, locus coeruleus; s.a., splice acceptor; SubCD, dorsal subcoeruleus; SubCV, ventral subcoeruleus; TH, tyrosine hydroxylase; wt, wild-type.

60% reduction of hippocampal NE in Cre-negative $Dbh^{flx/flx}$ mice relative to $Dbh^{wt/wt}$ mice (Figure 2B), demonstrating that the Dbh^{flx} allele is hypomorphic (exhibits less than wild-type activity). We also found that NE content was significantly higher in $Dbh^{wt/wt}$ and $Dbh^{flx/flx}$ male than in female mice (p = .003, sex × genotype interaction) (Figure 2B; Figure S2A). Because DBH converts DA to NE, we also examined DA content in the hippocampus and found that it was significantly increased in $Dbh^{flx/flx}$ and $Dbh^{LC\text{-}null}$ mice relative to $Dbh^{wt/wt}$ controls ($p < .0001$, main effect of genotype, two-way analysis of variance [ANOVA] with Tukey's test) (Figure 2B). Furthermore, DA in $Dbh^{LC\text{-}null}$ hippocampus was significantly higher

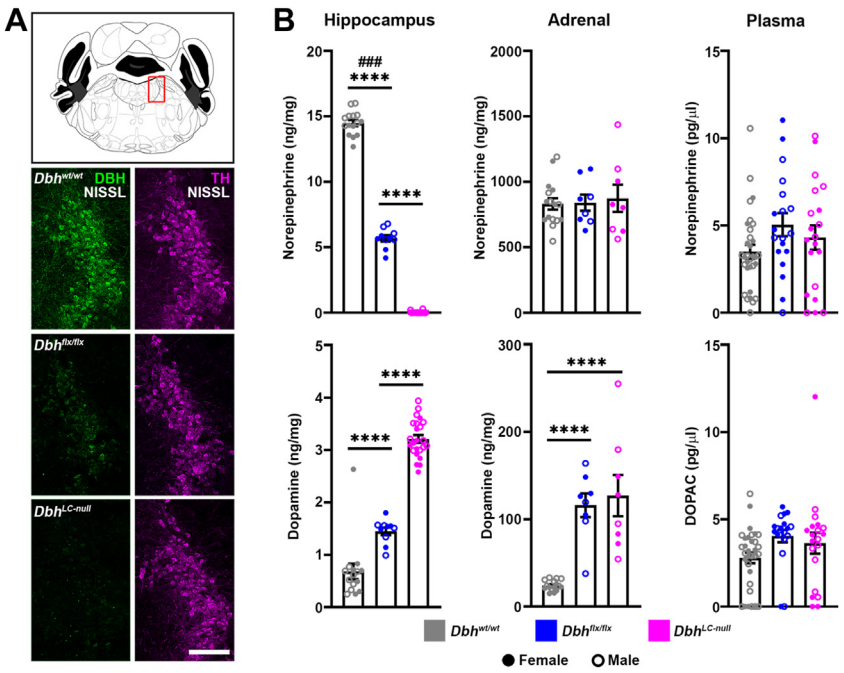

Figure 2. Disruption of norepinephrine synthesis in $Dbh^{LC\text{-}null}$ and $Dbh^{flx/flx}$ (Dbh^{hypo}) mice. **(A)** Coronal sections from $Dbh^{wt/wt}$, $Dbh^{flx/flx}$, and $Dbh^{LC\text{-}null}$ mice showing DBH (green) and/or TH (magenta) expression in the LC (representative images from n = 4 female and 4 male mice per genotype). Scale bar = 100 µm. **(B)** Levels of norepinephrine and dopamine or DOPAC in the hippocampus, adrenal, and plasma of $Dbh^{wt/wt}$, $Dbh^{flx/flx}$, and $Dbh^{LC\text{-}null}$ mice. Data are mean ± SEM. For hippocampus samples, n = 7 female (closed circles) and 8 male (open circles) $Dbh^{wt/wt}$ (includes 8 $En1^{Cre/wt}$ and 7 $En1^{wt/wt}$), 5 female and 5 male $Dbh^{flx/flx}$, and 11 female and 13 male $Dbh^{LC\text{-}null}$ mice. For adrenal, n = 8 female and 8 male $Dbh^{wt/wt}$ (8 $En1^{Cre/wt}$ and 7 $En1^{wt/wt}$), 4 female and 4 male $Dbh^{flx/flx}$, and 4 female and 4 male $Dbh^{LC\text{-}null}$ mice. For plasma samples, n = 14 female and 18 male $Dbh^{wt/wt}$ (17 $En1^{Cre/wt}$ and 15 $En1^{wt/wt}$), 10 female and 9 male $Dbh^{flx/flx}$, and 10 female and 10 male $Dbh^{LC\text{-}null}$ mice. $^{****}p < .0001$, $^{###}p = .0004$ (main effect of sex). LC, locus coeruleus; TH, tyrosine hydroxylase; wt, wild-type.

than in $Dbh^{flx/flx}$ ($p < .0001$, two-way ANOVA with Tukey's test) (Figure 2B), demonstrating that larger disruptions in NE synthesis corresponded to greater hippocampal DA levels. In contrast, we observed no genotype-specific differences in NE content in adrenal or release in plasma and no difference in levels of the DA metabolite DOPAC in plasma. However, DA was significantly increased in adrenal of both $Dbh^{flx/flx}$ and $Dbh^{LC\text{-}null}$ mice ($p < .0001$, two-way ANOVA with Tukey's test) (Figure 2B). Taken together with the results of the analysis of recombination (Figure 1), our findings confirm that $Dbh^{LC\text{-}null}$ mice lack NE synthesis in the LC and that the Dbh^{flx} allele is hypomorphic rather than functionally wild-type.

To explore possible causes of the unexpected hypomorphy of $Dbh^{flx/flx}$ mice (hereafter designated Dbh^{hypo}), we examined regulatory annotations for the mouse genome (GRCm39) in the Ensembl Genome Browser (Release 108) (34). We found that a 1399-bp putative enhancer region in mouse *Dbh* intron 1 (Ensembl ENSMUSR00000824281) is interrupted by the upstream loxP at an EcoRI site beginning at nucleotide 291. Disruption of an enhancer is expected to alter mRNA levels; therefore, we performed droplet digital PCR to assess Dbh mRNA in both the central and peripheral noradrenergic systems (Figure 3). We examined mRNA levels in the pons (which includes the LC, subcoeruleus, and A5 nuclei), medulla (A1 and A2 nuclei), adrenal, and stellate ganglion. In Dbh^{hypo} mice, we found reduced Dbh mRNA relative to wild-type in all tissues examined (reduction of approximately 73% in the pons, 64% in the medulla, 57% in adrenal, and 78% in the stellate ganglion). We also found a sex-specific difference in adrenal, with males having higher *Dbh* expression than females (p = .0010, main effect of sex) (Figure 3; Figure S2B). Next, we tested whether reduced *Dbh* expression affects *Th* and found no difference in *Th* mRNA expression between Dbh^{hypo} and $Dbh^{wt/wt}$ samples (Figure 3). Therefore, these data indicate that Dbh^{hypo} and $Dbh^{LC\text{-}null}$ mice represent 2 distinct models of disrupted *Dbh* expression.

Impaired Contextual Fear Response in Dbh^{hypo} and $Dbh^{LC\text{-}null}$ Mice

It has previously been shown that global loss of NE synthesis beginning in the early postnatal period results in deficits in hippocampus-dependent memory retrieval (11). To assess the effects of embryonic loss of LC-NE—both partial and complete—on behavior and NE and DA release dynamics, we used spectrally resolved fiber photometry (30) combined with contextual fear conditioning. Male and female $Dbh^{LC\text{-}null}$, Dbh^{hypo}, and $Dbh^{wt/wt}$ mice were injected with AAVs expressing tdTomato and either an NE sensor ($GRAB_{NE}$) (28) or a DA sensor ($GRAB_{DA}$) (29) and implanted with fiber optical probes in the hippocampal dCA1 (Figure 4A). Next, we utilized the preexposure-dependent contextual fear assay (Figure 4B), which consists of 4 phases. A preexposure phase allows the mice to explore the novel context and acquire a hippocampus-dependent contextual representation of the conditioning chamber. During the immediate-shock day, this contextual representation is rapidly retrieved and associated with the shock to form a contextual fear memory. Recent (24 hours after shock) and remote (2 weeks after shock) tests assess short- and long-term retrieval of the contextual fear memory, as measured by the amount of time that the mice spend freezing (i.e., motionless, a species-specific fear response) when placed back in the conditioning chamber.

During the preexposure phase of the test, we observed no genotype- or sex-specific differences in the distance moved, indicating no baseline differences in motor exploration

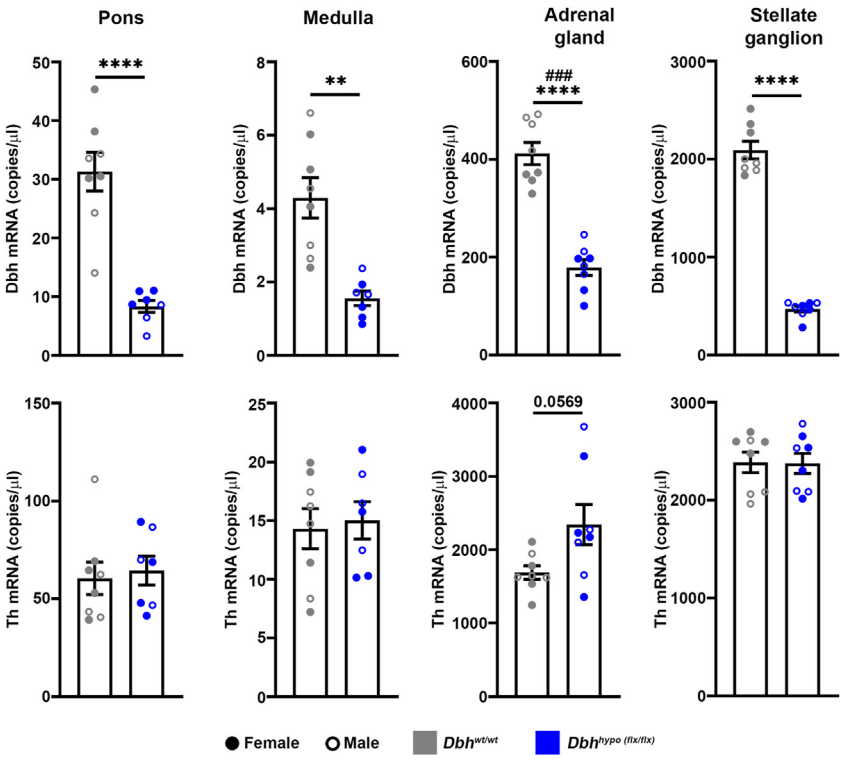

Figure 3. Dbh and Th mRNA levels in *Dbh*$^{wt/wt}$ and *Dbh*^{hypo} mice. Data are mRNA levels estimated by droplet digital polymerase chain reaction, mean ± SEM. For *Dbh*^{hypo} pons, n = 4 female (closed circles) and 3 male (open circles) mice. For all other samples, n = 4 female and 4 male mice. $^{****}p < .0001$, $^{**}p = .0020$, $^{###}p = .0010$ (main effect of sex). mRNA, messenger RNA; Th, tyrosine hydroxylase; wt, wild-type.

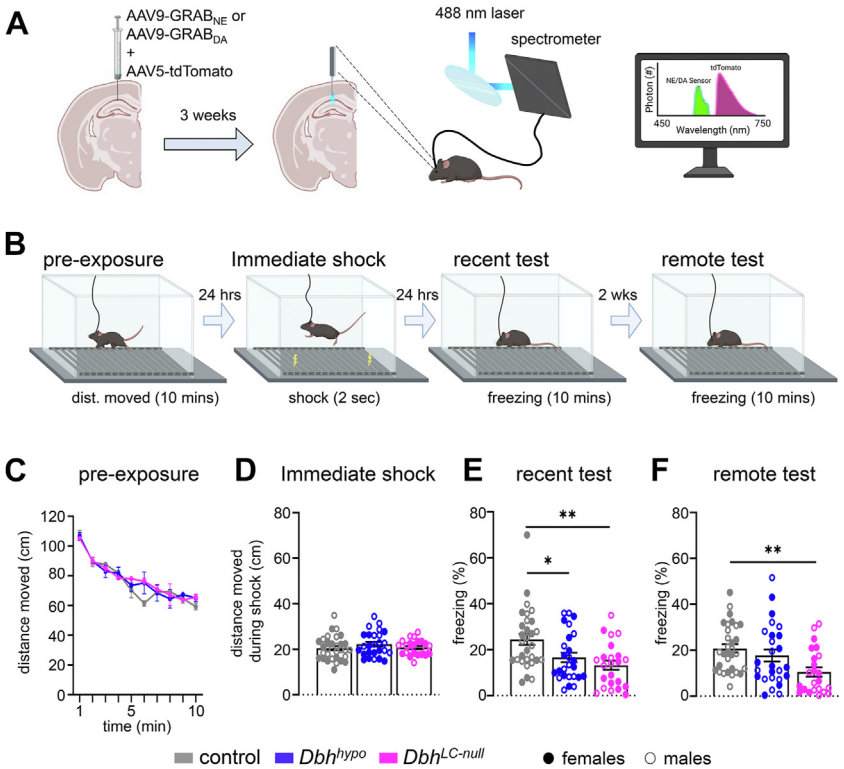

Figure 4. Experimental conditions and results of context-dependent fear conditioning. **(A)** Coronal schematic of mouse brain showing injection site of AAV9-GRAB$_{NE}$ or -GRAB$_{DA}$ and AAV5-tdTomato viruses in the dorsal CA1 region of the hippocampus. Fiber optic probes were implanted 3 weeks later above the dorsal CA1. In vivo fiber photometry recordings were performed using a spectrometer-based system with a 488-nm emission laser. Software allowed for simultaneous visualization of photon counts from fluorescent signals at various wavelengths. **(B)** Schematic of context-dependent fear conditioning paradigm performed in parallel with fiber photometry. **(C)** Distance the mice moved during the preexposure recording. **(D)** Distance moved during shock. **(E)** Percentage of time spent freezing during the recent context test ($^{**}p = .0021$, $^{*}p = .031$). **(F)** Freezing during the remote context test ($^{**}p = .0042$). Data are mean ± SEM. Two-way analysis of variance with Tukey's multiple comparisons test, n = 31 *Dbh*$^{wt/wt}$ control (15 female, 16 male), n = 26 *Dbh*^{hypo} (13 female, 13 male), and n = 23 *Dbh*$^{LC\text{-}null}$ (12 female, 11 male) mice. DA, dopamine; dist., distance; LC, locus coeruleus; NE, norepinephrine; wt, wild-type.

(Figure 4C). Similarly, no genotype-specific differences in distance moved were observed during the activity burst associated with the 2-second aversive foot shock (Figure 4D). However, males were observed to move more than females (p = .0090, main effect of sex) (Figure S2C). These results indicate that NE deficits associated with the *Dbh*^{hypo} and *Dbh*$^{LC\text{-}null}$ mouse models do not affect overall activity or sensitivity to aversive stimuli. To assess retrieval of contextual fear memory, we measured the percentage of time mice spent freezing when placed back in the chamber in which they received the shock. During the recent retrieval test, both *Dbh*^{hypo} and *Dbh*$^{LC\text{-}null}$ mice exhibited reduced freezing compared with controls (*Dbh*^{hypo}, p = .0305; *Dbh*$^{LC\text{-}null}$, p = .0021) (Figure 4E; Figure S3). However, during the remote retrieval test, only *Dbh*$^{LC\text{-}null}$ mice still exhibited significantly reduced freezing (p = .0042) (Figure 4F).

Dynamic Release of NE and DA in the dCA1 During Contextual Fear Conditioning

Next, we analyzed the fiber photometry data to assess NE and DA dynamics in the hippocampal dCA1 during the 4 phases of the fear conditioning paradigm. The photometry signal was aligned to aversive shock and to onset of immobility or freezing during the preexposure phase and tests of memory retrieval. During the preexposure, immobility was relatively rare and of shorter duration (average immobility bout length = 3.851 ± 0.51 seconds vs. freeze bout length for recent and remote context tests = 7.655 ± 0.78 seconds and 8.505 ± 0.65 seconds, respectively) but sufficient to permit analysis of event-triggered averages. We observed no genotype- or sex-specific differences in NE or DA release during immobility in the preexposure phase (Figure S4), consistent with our observation that *Dbh*$^{LC\text{-}null}$, *Dbh*^{hypo}, and littermate control mice have similar locomotion at baseline. However, during the aversive foot shock, we observed an immediate increase in NE release in both *Dbh*^{hypo} and control mice. As expected, the evoked increase in NE was absent in *Dbh*$^{LC\text{-}null}$ mice (Figure 5A, B), consistent with our measure of tissue content (Figure 2B). This result also serves as a negative control and confirms the specificity of the GRAB$_{NE}$ sensor. During the 10 seconds following the foot shock, NE release was significantly increased in both wild-type controls (p = .0009) and *Dbh*^{hypo} mice (p = .0384) compared with *Dbh*$^{LC\text{-}null}$ mice (Figure 5C). We also observed increased DA release in response to the shock (Figure 5A, D), with release in *Dbh*$^{LC\text{-}null}$ mice significantly greater than in *Dbh*^{hypo} mice (p = .0067) and wild-type controls (p < .0001) (Figure 5E). Despite the significant difference in NE

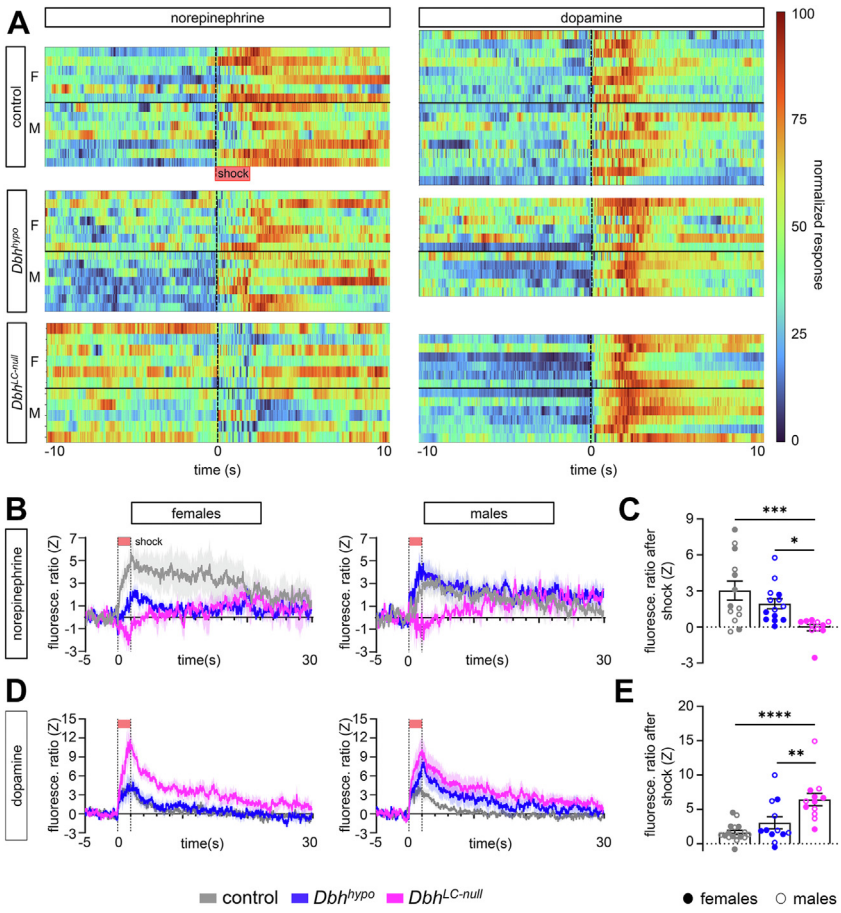

Figure 5. Norepinephrine and dopamine dynamics in the dorsal CA1 during and immediately following a noxious foot shock. **(A)** GRAB$_{NE}$/tdTomato (norepinephrine) and GRAB$_{DA}$/tdTomato (dopamine) fluorescence ratios expressed as a normalized response aligned to foot shock (dotted line). Each row in the heat map corresponds to an individual mouse, with the largest ratio for that mouse set to 100 and the smallest ratio set to 0. **(B)** Average GRAB$_{NE}$/tdTomato fluorescence ratios aligned to shock in female (left) and male (right) *Dbh*$^{wt/wt}$ control, *Dbh*^{hypo}, and *Dbh*$^{LC\text{-}null}$ mice. **(C)** Average norepinephrine response during the first 10 seconds after the foot shock for the *Dbh*$^{wt/wt}$ control (95% CI of mean, 1.31 to 4.76), *Dbh*^{hypo} (1.03 to 2.83), and *Dbh*$^{LC\text{-}null}$ mice (−0.64 to 0.56; encompasses 0). ***p = .0009, *p = .0384. **(D)** Average GRAB$_{DA}$/tdTomato fluorescence ratios aligned to shock. **(E)** Average dopamine response during the first 10 seconds after shock for the *Dbh*$^{wt/wt}$ control (95% CI of mean, 0.98 to 2.30), *Dbh*^{hypo} (1.10 to 4.99), and *Dbh*$^{LC\text{-}null}$ mice (4.41 to 8.44). **p = .0067, ****p < .0001. GRAB$_{NE}$ cohort: n = 13 *Dbh*$^{wt/wt}$ control (6 female, 7 male), n = 14 *Dbh*^{hypo} (7 female, 7 male), and n = 11 *Dbh*$^{LC\text{-}null}$ (6 female, 5 male) mice. GRAB$_{DA}$ cohort: n = 17 *Dbh*$^{wt/wt}$ control (8 female, 9 male), n = 12 *Dbh*^{hypo} (6 female, 6 male), and n = 12 *Dbh*$^{LC\text{-}null}$ (6 female, 6 male) mice. LC, locus coeruleus; wt, wild-type.

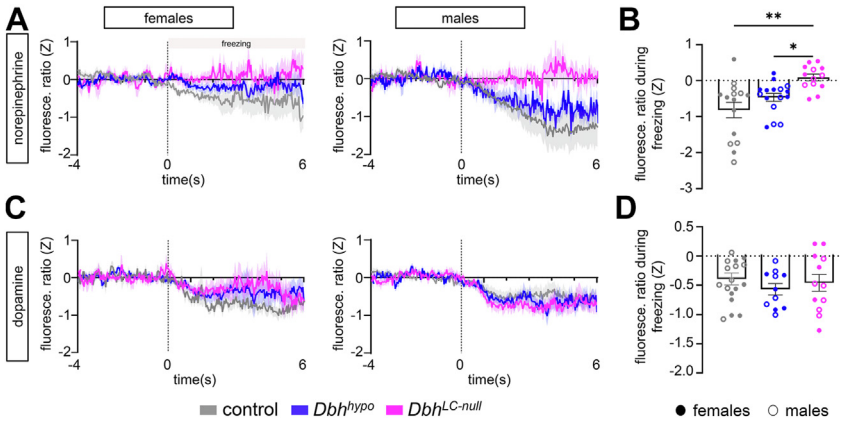

Figure 6. Norepinephrine and dopamine dynamics in the dorsal CA1 during freezing in the recent context test. **(A)** Average $GRAB_{NE}$/tdTomato fluorescence ratios aligned to freezing in female (left) and male (right) $Dbh^{wt/wt}$, Dbh^{hypo}, and $Dbh^{LC\text{-}null}$ mice. **(B)** Averages of norepinephrine response during the first 6 seconds of freezing episodes in $Dbh^{wt/wt}$ control (95% CI of mean, −1.3 to −0.36), Dbh^{hypo} (−0.70 to −0.23), and $Dbh^{LC\text{-}null}$ mice (−0.12 to 0.29; encompasses 0). $^{**}p$ = .0003, $^{*}p$ = .0384. **(C)** Average $GRAB_{DA}$/tdTomato fluorescence ratios aligned to freezing. **(D)** Average dopamine responses during the first 6 seconds of freezing episodes in $Dbh^{wt/wt}$ control (95% CI of mean, −0.61 to −0.18), Dbh^{hypo} (−0.78 to −0.35), and $Dbh^{LC\text{-}null}$ mice (−0.77 to −0.14). Data are mean ± SEM. Two-way analysis of variance with Tukey's test. $GRAB_{NE}$ cohort: n = 13 $Dbh^{wt/wt}$ control (6 female, 7 male), n = 14 Dbh^{hypo} (7 female, 7 male), and n = 11 $Dbh^{LC\text{-}null}$ mice (6 female, 5 male). $GRAB_{DA}$ cohort: n = 18 $Dbh^{wt/wt}$ control (9 female, 9 male), n = 12 Dbh^{hypo} (6 female, 6 male), and n = 12 $Dbh^{LC\text{-}null}$ mice (6 female, 6 male). LC, locus coeruleus; wt, wild-type.

and DA tissue content between Dbh^{hypo} and wild-type mice (Figure 2B), we found no significant differences in NE or DA release between those 2 genotypes (Figure 5C, E). However, we did note a trend for a genotype × sex interaction for NE release (p = .059, two-way ANOVA) in which fluorescence ratios from male Dbh^{hypo} mice resembled those from wild-type males and female Dbh^{hypo} mice resembled female $Dbh^{LC\text{-}null}$ mice (Figure 5B, C; Figure S2D).

Next, we assessed NE and DA release in the dCA1 during freezing in the recent (24 hours after shock) and remote (2 weeks after shock) tests, which assess short- and long-term retrieval of the contextual fear memory. Both Dbh^{hypo} mice (p = .0384) and wild-type controls (p = .0003) exhibited significantly decreased NE release during freezing in the recent test (Figure 6A, B). As expected, we observed no change in NE release in $Dbh^{LC\text{-}null}$ mutants (Figure 6A, B). To examine the relationship between the decrease in NE signal and the length of a freezing bout, we used a general linear model. We found that longer freezing bouts predicted a larger freezing-related drop in NE signal in males (main effect of bout length in males and females, $p < .001$ and p = .225, respectively) (Figure S5). DA release was also decreased during freezing in the recent test; however, this decrease occurred in all genotypes including $Dbh^{LC\text{-}null}$ mice, and there was no significant difference between the groups (Figure 6C, D). We found no relationship between DA signal and length of freezing (main effect of bout length in males and females, p = .676 and p = .585, respectively) (Figure S5).

We observed no genotype-specific decrease in NE release during freezing in the remote test of long-term retrieval (Figure 7A, B), although male mice exhibited a significant decrease relative to females (p = .0484, main effect of sex, two-way ANOVA with Tukey's test). Consistent with the recent test, DA release was decreased in all mice during freezing in the remote test, with no significant difference found between the groups (Figure 7C, D). We found no relationship between length of freezing and either NE signal or DA signal (Figure S5). Next, we examined whether NE or DA release in response to the shock predicted subsequent freezing behavior in the recent and remote context tests. DA, but not NE, showed a significant

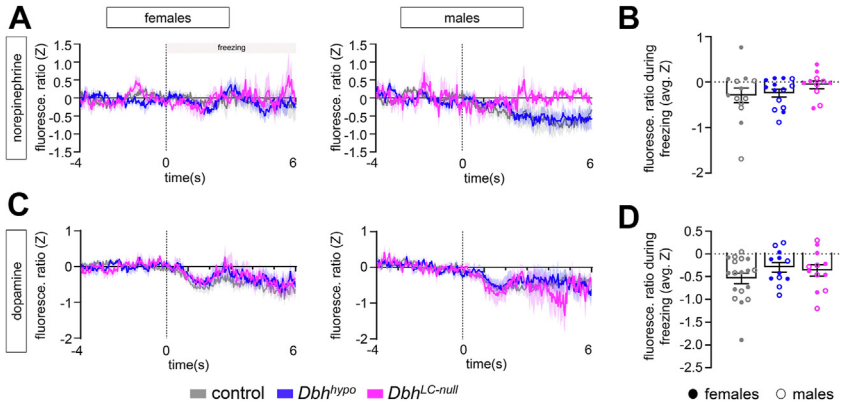

Figure 7. Norepinephrine and dopamine dynamics in the dorsal CA1 during freezing in the remote context test. **(A)** Average $GRAB_{NE}$/tdTomato fluorescence ratios aligned to freezing in female (left) and male (right) control, Dbh^{hypo}, and $Dbh^{LC\text{-}null}$ mice. **(B)** Average norepinephrine response during the first 6 seconds of freezing in $Dbh^{wt/wt}$ control (95% CI of mean, −0.64 to 0.057), Dbh^{hypo} (−0.43 to −0.06), and $Dbh^{LC\text{-}null}$ mice (−0.25 to 0.13). **(C)** Average $GRAB_{DA}$/tdTomato fluorescence ratios aligned to freezing. **(D)** Average dopamine responses during the first 6 seconds of freezing episodes in $Dbh^{wt/wt}$ control (95% CI of mean, −0.78 to −0.29), Dbh^{hypo} (−0.53 to −0.063), and $Dbh^{LC\text{-}null}$ mice (−0.64 to −0.087). Data are mean ± SEM. Two-way analysis of variance with Tukey's test. $GRAB_{NE}$ cohort: n = 12 $Dbh^{wt/wt}$ control (5 female, 7 male), n = 14 Dbh^{hypo} (7 female, 7 male), and n = 11 $Dbh^{LC\text{-}null}$ (6 female, 5 male) mice. $GRAB_{DA}$ cohort: n = 18 $Dbh^{wt/wt}$ control (9 female, 9 male), n = 12 Dbh^{hypo} (6 female, 6 male), and n = 12 $Dbh^{LC\text{-}null}$ (6 female, 6 male) mice. Avg., average; fluoresce., fluorescence; LC, locus coeruleus; wt, wild-type.

predictive relationship in all genotypes examined, and this was driven by the female mice (sustained shock response coefficient in females, $p = .003$ and $p = .001$ for recent and remote, respectively) (Figure S6).

Finally, we performed additional analyses to clarify the specific relationship between freezing behavior and catecholamine release. A repeated measures analysis of freezing behavior and DA and NE release confirmed that the decrease in NE during freezing was specific to the recent test and showed that there were no differences in freezing between the recent and remote tests (Figure S7). We also found no relationship between locomotor activity and NE or DA release (Figure S8). Together with the lack of change in release during immobility in the preexposure phase (Figure S4), this analysis suggests that the decreased release is specific to freezing and not a general consequence of reduced locomotion.

Overall, these data identify unique patterns of NE and DA release dynamics in the dCA1 during the contextual fear assay that are differentially sensitive to partial or complete embryonic loss of NE.

DISCUSSION

Here, we describe 2 new mouse models of disrupted *Dbh* expression beginning prenatally: a fortuitous hypomorphic allele, Dbh^{hypo}, with reduced *Dbh* expression in noradrenergic neurons and an LC conditional knockout, $Dbh^{LC\text{-}null}$, with total loss of *Dbh* expression in the LC and reduced expression in other noradrenergic nuclei. Despite reduced Dbh mRNA expression in the adrenal and stellate ganglion of both mutants, NE content in the adrenal and release in the plasma was unchanged. Surprisingly, we did find an accumulation of DA in the adrenal which was not accompanied by any change in Th mRNA expression. Our new mouse lines will be useful tools to uncover the biochemical mechanisms behind these interesting differences and reveal important details of catecholamine biosynthesis in the central and peripheral noradrenergic systems. Regardless, our current findings indicate that monitoring of plasma NE as a proxy for brain NE levels should be approached with caution.

Using our new models of disrupted *Dbh* expression to link catecholamine dynamics with specific outcomes in the context-dependent fear conditioning paradigm, we found deficits in freezing and unique patterns of catecholamine release dynamics in the dCA1 that are differentially sensitive to partial or complete embryonic loss of NE. During acquisition of the contextual fear memory and the 10 seconds immediately following the shock, NE and DA release was increased in the dCA1 of both wild-type and Dbh^{hypo} mice. Although we found ~61% reduction in NE and ~113% increase in DA tissue content in the hippocampus of Dbh^{hypo} mice, we observed no significant difference in either NE or DA release compared with wild-type controls. DA release was only significantly increased in the total absence of NE release in the dCA1 of $Dbh^{LC\text{-}null}$ mutants.

The absence of increased DA release in the dCA1 of Dbh^{hypo} mice, despite the significant increase in tissue content, highlights the tight regulation of release dynamics. The increase in DA tissue content was found in the hippocampus of both *Dbh* mutants and was inversely proportional to deficits in NE content, suggesting that the increase is a direct result of decreased conversion of DA to NE in the LC. Several studies have shown that LC neurons are capable of releasing DA when artificially stimulated (35,36), but other experiments suggest that midbrain dopaminergic neurons are the most likely natural source of DA in the dorsal CA1 (14). Our data do not reveal the origin of the increased DA release observed in $Dbh^{LC\text{-}null}$ mice. Although it is plausibly due to an accumulation of DA in LC neurons, it could also be an indirect response of midbrain dopaminergic neurons to decreased LC-NE signaling.

The large release of DA and NE in response to the foot shock observed in wild-type mice argues that the dorsal hippocampus is powerfully modulated by the aversive unconditioned stimulus. While the increase in NE release is consistent with previous studies that have examined the LC response to noxious stimuli (37–42), the increase in both catecholamines has important implications for theories of dorsal hippocampal involvement in contextual fear. Modulation of the hippocampus by shock-induced DA and NE release may serve to strengthen and/or modify the contextual representation, consistent with previous work showing that shock presentation causes remapping of place cells (43,44). In addition, there is some evidence that the shock itself may become integrated into the contextual representation directly, which is thought to play an important role in fear extinction (45), a process that is strongly modulated by LC-NE signaling (41,46).

In $Dbh^{LC\text{-}null}$ mice, the observed increase in DA release during foot shock could contribute to behavioral changes, potentially compensating for the loss of LC-NE in some aspects of behavior and/or exacerbating others. These effects may be complicated by hypersensitivity to DA signaling, a previously reported consequence of *Dbh* loss (47,48). Methods to selectively manipulate DA and NE during initial formation of the contextual representation, the context-shock association, consolidation, and retrieval will be required to determine which of these phases of learning are most impacted by DA and NE neuromodulation.

The observed reduction in NE release during freezing is interesting considering that increasing LC activity leads to expression of anxiety-related behaviors and is aversive (49,50). A possible unifying explanation comes from findings that lower levels of tonic LC activity enhance signal detection and behavioral performance in attentionally demanding tasks (51). In contrast, higher tonic LC activity may facilitate evaluation of the sensory environment that is more appropriate in new and uncertain conditions (51). Thus, what we may be observing during expression of freezing is a shift from higher tonic activity during exploration of the environment to a lower level of tonic activity that enhances detection of threat (52).

Comparisons of the *Dbh* mouse models used in the current study with a full-body Dbh^{ko} (22) indicate that freezing is sensitive to levels of NE and the timing of the insult. The reduced freezing in the recent but not the remote test exhibited by Dbh^{hypo} mice is similar to the phenotype of the full-body Dbh^{ko} mice, which also have a deficit in recent but not remote retrieval (53), suggesting that NE is not required at remote time points when contextual fear memories have already gone through a systems consolidation process. However, the deficits in freezing at both recent and remote time points found in $Dbh^{LC\text{-}null}$ mutants may suggest a more

critical role for LC-NE in remote retrieval. Alternatively, the data may indicate a more complex role for LC-NE that involves other aspects of the fear response or general sensory information processing.

The phenotypic differences between the mouse models may be at least partially due to differences in NE levels during prenatal development. $Dbh^{LC\text{-}null}$ mice lack LC-NE throughout prenatal and postnatal development, while Dbh^{hypo} mice have at least partial NE synthesis during embryonic development. Similarly, Dbh^{ko} mice have low levels of prenatal NE synthesis resulting from prenatal L-DOPS treatment to avoid the embryonic lethal effect of total NE loss (22). It is possible that these early development differences in NE levels differentially affect other important brain regions such as the amygdala and prefrontal cortex. Behavior in the mutants may also be modulated by differences in *Dbh* expression, and subsequent NE and epinephrine production, in the periphery (54). Peripheral *Dbh* expression is eliminated postnatally in Dbh^{ko} mice but present, although at reduced levels, in both of the new models. Alternatively, the behavioral differences among *Dbh* mutants may result from differences in background strain, the specific molecular defect, or the fear conditioning protocol. Future work will be necessary to untangle these competing hypotheses.

Several sex differences observed in this study (Figure S3) are worth highlighting given the well-established sex differences in NE signaling (55). Wild-type males showed higher NE levels in the hippocampus and higher *Dbh* expression in adrenal. We also found that Dbh^{hypo} and wild-type males showed a more robust drop in NE during freezing that was predicted by the length of the freezing bout. In addition, we observed a sex interaction in Dbh^{hypo} mice wherein males showed similar levels of shock-induced NE release to controls, and females more closely resembled $Dbh^{LC\text{-}null}$ mutants (Figure S2D). Lastly, the predictive correlation between shock-induced DA release and subsequent freezing behavior was driven by the females (Figure S6). These findings suggest a complex relationship between sex, NE, and DA dynamics and partial versus complete loss of NE production. Our findings also highlight the critical importance of conducting sufficiently powered, sex-balanced photometry studies so that these sex interactions can be uncovered. Determining whether the sex differences have a single underlying cause or multiple causes—possibly including sex hormones, epigenetics, differing expression levels of receptors or other genes involved in catecholamine metabolism—will require a focused analysis.

ACKNOWLEDGMENTS AND DISCLOSURES

This work was supported by the Intramural Research Program at the National Institute of Environmental Health Sciences (NIEHS) (Grant Nos. ZIA ES102805 [to PJ] and ZIC ES103330) and by the Extramural Research Program at the National Institute of Diabetes and Digestive and Kidney Diseases (Grant No. R00 DK119586 [to NRS]).

We thank Caroll Co and Katherine Allen (DLH) for their statistical expertise in the correlations and general linear model analyses and Sandra McBride and Matthew Bridge (DLH) for the custom R code used to analyze photometry data. Their contributions were supported by the NIEHS under contract GS-00F-173CA-75N96021F00109 to Social and Scientific Systems, Inc., a DLH Holdings Corp Company. We also thank Wesley Gladwell and Kevin Gerrish (NIEHS Molecular Genomics Core Facility) for performing droplet digital PCR and the Vanderbilt Neurochemistry Core for catecholamine mass spectrometry. Valuable support was also provided by the NIEHS Comparative Medicine Branch and the Neurobehavioral, Fluorescence Microscopy and Imaging, and Viral Vector Cores. We thank Dr. Guohong Cui for valuable discussion of the photometry data.

A previous version of this article was published as a preprint on bioRxiv: https://doi.org/10.1101/2023.03.26.534277.

The authors report no biomedical financial interests or potential conflicts of interest.

ARTICLE INFORMATION

From the Neurobiology Laboratory, NIEHS, National Institutes of Health, Department of Health and Human Services, Research Triangle Park, North Carolina (LRW, NWP, IYE, DP, CLS, KGS, ALD, VWK, PJ); Neurobehavioral Core Laboratory, NIEHS, National Institutes of Health, Department of Health and Human Services, Research Triangle Park, North Carolina (LRW, SAF, SP, JDC); Social and Scientific Systems, Inc., a DLH Holdings Corp Company, Durham, North Carolina (KSK); and the Department of Physiology and Neurobiology, Department of Biomedical Engineering, Institute for System Genomics, Connecticut Institute for the Brain & Cognitive Sciences, University of Connecticut, Storrs, Connecticut (NRC).

LRW and NWP contributed equally to this article.

Address correspondence to Jesse D. Cushman, Ph.D., at jesse.cushman@nih.gov, or Patricia Jensen, Ph.D., at patricia.jensen@nih.gov.

Received Apr 12, 2023; revised Sep 28, 2023; accepted Oct 5, 2023.

Supplementary material cited in this article is available online at https://doi.org/10.1016/j.bpsgos.2023.10.001.

REFERENCES

1. Bast T (2007): Toward an integrative perspective on hippocampal function: From the rapid encoding of experience to adaptive behavior. Rev Neurosci 18:253–281.
2. Rudy JW, O'Reilly RC (1999): Contextual fear conditioning, conjunctive representations, pattern completion, and the hippocampus. Behav Neurosci 113:867–880.
3. Smith DM, Bulkin DA (2014): The form and function of hippocampal context representations. Neurosci Biobehav Rev 40:52–61.
4. Cushman JD, Fanselow MS (2012): Context fear learning. In: Seel NM, editor. Encyclopedia of the Sciences of Learning. Boston, MA: Springer, 797–799.
5. Krasne FB, Cushman JD, Fanselow MS (2015): A Bayesian context fear learning algorithm/automaton. Front Behav Neurosci 9:112.
6. Sanders MJ, Wiltgen BJ, Fanselow MS (2003): The place of the hippocampus in fear conditioning. Eur J Pharmacol 463:217–223.
7. Kim JJ, Fanselow MS (1992): Modality-specific retrograde amnesia of fear. Science 256:675–677.
8. Phillips RG, LeDoux JE (1992): Differential contribution of amygdala and hippocampus to cued and contextual fear conditioning. Behav Neurosci 106:274–285.
9. Chowdhury A, Luchetti A, Fernandes G, Filho DA, Kastellakis G, Tzilivaki A, *et al.* (2022): A locus coeruleus-dorsal CA1 dopaminergic circuit modulates memory linking. Neuron 110:3374–3388.e8.
10. Giustino TF, Maren S (2018): Noradrenergic modulation of fear conditioning and extinction. Front Behav Neurosci 12:43.
11. Murchison CF, Zhang XY, Zhang WP, Ouyang M, Lee A, Thomas SA (2004): A distinct role for norepinephrine in memory retrieval. Cell 117:131–143.
12. Seo DO, Zhang ET, Piantadosi SC, Marcus DJ, Motard LE, Kan BK, *et al.* (2021): A locus coeruleus to dentate gyrus noradrenergic circuit modulates aversive contextual processing. Neuron 109:2116–2130.e6.
13. Shen W, Chen S, Xiang Y, Yao Z, Chen Z, Wu X, *et al.* (2021): Astroglial adrenoreceptors modulate synaptic transmission and contextual fear memory formation in dentate gyrus. Neurochem Int 143:104942.
14. Tsetsenis T, Badyna JK, Wilson JA, Zhang X, Krizman EN, Subramaniyan M, *et al.* (2021): Midbrain dopaminergic innervation of the hippocampus is sufficient to modulate formation of aversive memories. Proc Natl Acad Sci USA 118:e2111069118.

15. Tsetsenis T, Broussard JI, Dani JA (2022): Dopaminergic regulation of hippocampal plasticity, learning, and memory. Front Behav Neurosci 16:1092420.
16. Wagatsuma A, Okuyama T, Sun C, Smith LM, Abe K, Tonegawa S (2018): Locus coeruleus input to hippocampal CA3 drives single-trial learning of a novel context. Proc Natl Acad Sci USA 115:E310–E316.
17. Plummer NW, Evsyukova IY, Robertson SD, de Marchena J, Tucker CJ, Jensen P (2015): Expanding the power of recombinase-based labeling to uncover cellular diversity. Development 142:4385–4393.
18. Robertson SD, Plummer NW, de Marchena J, Jensen P (2013): Developmental origins of central norepinephrine neuron diversity. Nat Neurosci 16:1016–1023.
19. Lee HS, Han JH (2023): Activity patterns of individual neurons and ensembles correlated with retrieval of a contextual memory in the dorsal CA1 of mouse hippocampus. J Neurosci 43:113–124.
20. Tanaka KZ, Pevzner A, Hamidi AB, Nakazawa Y, Graham J, Wiltgen BJ (2014): Cortical representations are reinstated by the hippocampus during memory retrieval. Neuron 84:347–354.
21. Tsetsenis T, Badyna JK, Li R, Dani JA (2022): Activation of a locus coeruleus to dorsal hippocampus noradrenergic circuit facilitates associative learning. Front Cell Neurosci 16:887679.
22. Thomas SA, Matsumoto AM, Palmiter RD (1995): Noradrenaline is essential for mouse fetal development. Nature 374:643–646.
23. Rudy JW, Huff NC, Matus-Amat P (2004): Understanding contextual fear conditioning: Insights from a two-process model. Neurosci Biobehav Rev 28:675–685.
24. Stote DL, Fanselow MS (2004): NMDA receptor modulation of incidental learning in Pavlovian context conditioning. Behav Neurosci 118:253–257.
25. George SH, Gertsenstein M, Vintersten K, Korets-Smith E, Murphy J, Stevens ME, *et al.* (2007): Developmental and adult phenotyping directly from mutant embryonic stem cells. Proc Natl Acad Sci USA 104:4455–4460.
26. Sciolino NR, Hsiang M, Mazzone CM, Wilson LR, Plummer NW, Amin J, *et al.* (2022): Natural locus coeruleus dynamics during feeding. Sci Adv 8:eabn9134.
27. Oh SW, Harris JA, Ng L, Winslow B, Cain N, Mihalas S, *et al.* (2014): A mesoscale connectome of the mouse brain. Nature 508:207–214.
28. Feng J, Zhang C, Lischinsky JE, Jing M, Zhou J, Wang H, *et al.* (2019): A genetically encoded fluorescent sensor for rapid and specific in vivo detection of norepinephrine. Neuron 102:745–761.e8.
29. Sun F, Zhou J, Dai B, Qian T, Zeng J, Li X, *et al.* (2020): Next-generation GRAB sensors for monitoring dopaminergic activity in vivo. Nat Methods 17:1156–1166.
30. Meng C, Zhou J, Papaneri A, Peddada T, Xu K, Cui G (2018): Spectrally resolved fiber photometry for multi-component analysis of brain circuits. Neuron 98:707–717.e4.
31. Thomas SA, Marck BT, Palmiter RD, Matsumoto AM (1998): Restoration of norepinephrine and reversal of phenotypes in mice lacking dopamine beta-hydroxylase. J Neurochem 70:2468–2476.
32. Lewandoski M, Meyers EN, Martin GR (1997): Analysis of FGF8 gene function in vertebrate development. Cold Spring Harb Symp Quant Biol 62:159–168.
33. Kimmel RA, Turnbull DH, Blanquet V, Wurst W, Loomis CA, Joyner AL (2000): Two lineage boundaries coordinate vertebrate apical ectodermal ridge formation. Genes Dev 14:1377–1389.
34. Cunningham F, Allen JE, Allen J, Alvarez-Jarreta J, Amode MR, Armean IM, *et al.* (2022): Ensembl 2022. Nucleic Acids Res 50:D988–D995.
35. Kempadoo KA, Mosharov EV, Choi SJ, Sulzer D, Kandel ER (2016): Dopamine release from the locus coeruleus to the dorsal hippocampus promotes spatial learning and memory. Proc Natl Acad Sci USA 113:14835–14840.
36. Takeuchi T, Duszkiewicz AJ, Sonneborn A, Spooner PA, Yamasaki M, Watanabe M, *et al.* (2016): Locus coeruleus and dopaminergic consolidation of everyday memory. Nature 537:357–362.
37. Cedarbaum JM, Aghajanian GK (1978): Activation of locus coeruleus neurons by peripheral stimuli: Modulation by a collateral inhibitory mechanism. Life Sci 23:1383–1392.
38. Devilbiss DM, Berridge CW (2006): Low-dose methylphenidate actions on tonic and phasic locus coeruleus discharge. J Pharmacol Exp Ther 319:1327–1335.
39. Mana MJ, Grace AA (1997): Chronic cold stress alters the basal and evoked electrophysiological activity of rat locus coeruleus neurons. Neuroscience 81:1055–1064.
40. Neves RM, van Keulen S, Yang M, Logothetis NK, Eschenko O (2018): Locus coeruleus phasic discharge is essential for stimulus-induced gamma oscillations in the prefrontal cortex. J Neurophysiol 119:904–920.
41. Uematsu A, Tan BZ, Ycu EA, Cuevas JS, Koivumaa J, Junyent F, *et al.* (2017): Modular organization of the brainstem noradrenaline system coordinates opposing learning states. Nat Neurosci 20:1602–1611.
42. Valentino RJ, Foote SL (1988): Corticotropin-releasing hormone increases tonic but not sensory-evoked activity of noradrenergic locus coeruleus neurons in unanesthetized rats. J Neurosci 8:1016–1025.
43. Moita MA, Rosis S, Zhou Y, LeDoux JE, Blair HT (2004): Putting fear in its place: Remapping of hippocampal place cells during fear conditioning. J Neurosci 24:7015–7023.
44. Ormond J, Serka SA, Johansen JP (2023): Enhanced reactivation of remapping place cells during aversive learning. J Neurosci 43:2153–2167.
45. Lacagnina AF, Brockway ET, Crovetti CR, Shue F, McCarty MJ, Sattler KP, *et al.* (2019): Distinct hippocampal engrams control extinction and relapse of fear memory. Nat Neurosci 22:753–761.
46. Giustino TF, Ramanathan KR, Totty MS, Miles OW, Maren S (2020): Locus coeruleus norepinephrine drives stress-induced increases in basolateral amygdala firing and impairs extinction learning. J Neurosci 40:907–916.
47. Schank JR, Ventura R, Puglisi-Allegra S, Alcaro A, Cole CD, Liles LC, *et al.* (2006): Dopamine beta-hydroxylase knockout mice have alterations in dopamine signaling and are hypersensitive to cocaine. Neuropsychopharmacology 31:2221–2230.
48. Weinshenker D, Schroeder JP (2007): There and back again: A tale of norepinephrine and drug addiction. Neuropsychopharmacology 32:1433–1451.
49. McCall JG, Al-Hasani R, Siuda ER, Hong DY, Norris AJ, Ford CP, Bruchas MR (2015): CRH engagement of the locus coeruleus noradrenergic system mediates stress-induced anxiety. Neuron 87:605–620.
50. Sciolino NR, Plummer NW, Chen YW, Alexander GM, Robertson SD, Dudek SM, *et al.* (2016): Recombinase-dependent mouse lines for chemogenetic activation of genetically defined cell types. Cell Rep 15:2563–2573.
51. Usher M, Cohen JD, Servan-Schreiber D, Rajkowski J, Aston-Jones G (1999): The role of locus coeruleus in the regulation of cognitive performance. Science 283:549–554.
52. Roelofs K, Dayan P (2022): Freezing revisited: Coordinated autonomic and central optimization of threat coping. Nat Rev Neurosci 23:568–580.
53. Murchison CF, Schutsky K, Jin SH, Thomas SA (2011): Norepinephrine and β_1-adrenergic signaling facilitate activation of hippocampal CA1 pyramidal neurons during contextual memory retrieval. Neuroscience 181:109–116.
54. McGaugh JL, Roozendaal B (2002): Role of adrenal stress hormones in forming lasting memories in the brain. Curr Opin Neurobiol 12:205–210.
55. Bangasser DA, Wiersielis KR, Khantsis S (2016): Sex differences in the locus coeruleus-norepinephrine system and its regulation by stress. Brain Res 1641:177–188.
56. Trichas G, Begbie J, Srinivas S (2008): Use of the viral 2A peptide for bicistronic expression in transgenic mice. BMC Biol 6:40.